Title

Characterizing the Force-Motion Tradeoff in Body-Powered Transmission Design

Authors

Abbott, Michael
Stuart, Hannah

Publication Date

2023-04-11

DOI

10.36227/techrxiv.22583827.v1

Characterizing the Force-Motion Tradeoff in Body-Powered Transmission Design

Michael E. Abbott, *Graduate Student Member, IEEE*, and Hannah S. Stuart, *Senior Member, IEEE*

***Abstract*— Upper-limb prosthesis users continue to reject devices despite continued research efforts. Today, the passive topology of body-powered prehensors, which physically transmits grasp force and position data between user and device, results in improved performance over myoelectric alternatives. However, the loads and postures on the user's body also result in discomfort, fatigue, and worsened grasp force control. Despite the long history and everyday adoption of body-powered prehensors in society, the measurement of how specific body loads and postures affect grasp performance and user experience has yet to be systematically studied. In this work, we present a body-powered prosthesis emulator to independently change required input forces and motions to study the positive and negative effects provided by the inherent haptic feedback. Using a simulated grasping task, we collect functional and qualitative data from 15 participants using a shoulder harness interface. Outcomes show that lowering required input motions and forces independently reduces negative outcomes, with diminishing returns below 1:1 output mappings. Given the tradeoff between force and motion in traditional body-powered transmissions, a transmission ratio of 1:1 balances both requirements. The purpose of this study is to inform future prehensor designs that leverage the transparency of body-power to deliver high functionality while mitigating user discomfort.**

***Index Terms*— Body-powered, prostheses, haptics.**

I. Introduction

LOSS of a hand diminishes a person's ability to complete activities of daily living [1], [2]. Despite substantial research efforts directed at this issue, users still remain unsatisfied with current upper-limb prosthetic solutions, abandoning between 33% and 50% of devices [3]. These individuals typically choose between two main classes of prostheses: body-powered (BP) and myoelectric, each with their own tradeoffs in terms of weight, functionality, and aesthetics.

Myoelectric prostheses measure muscle activity using surface electromyography (sEMG) electrodes embedded in the prosthetic socket to drive an active robotic end-effector. Such a system enables high degree of freedom dexterous control with multiple grasping postures and modes, such as in the beBionic [4] and iLimb Ultra [5] hands, though the efficacy of multi-grasp hands has not yet been established [6]. Myoelectric users frequently rate a lack of perceptual feedback and predictable control as barriers to adoption [7]. Some works include haptic feedback as add-ons to myoelectric devices through sensory substitution [8], [9] and modality matched [10], [11] methods, and recent prostheses have begun to include haptic feedback, such as the PSYONIC Ability Hand [12] released in 2021, though such feedback has yet to see widespread adoption.

Body-powered hand prostheses commonly feature a passive end-effector connected to a harness worn on the contralateral shoulder by a Bowden cable, as shown in Figure 1. This mechanical link transparently transmits forces and motions between user and device in a control topology formalized as

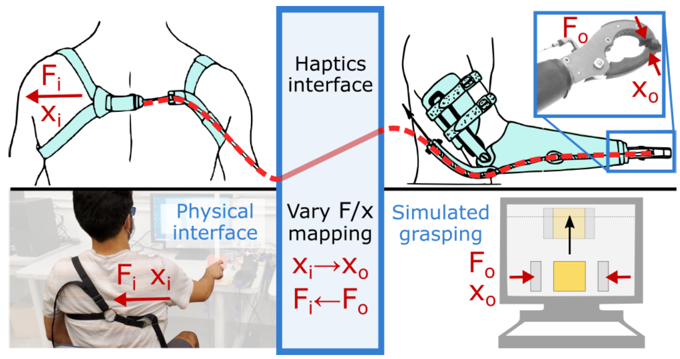

Fig. 1. In a body-powered device, input force F_i and input excursion x_i are mapped through a passive transmission to apply output force F_o and output motion x_o. To emulate a shoulder-driven prosthetic prehensor, our study is performed using a physical shoulder harness interface through which x_i is applied by a human subject. Resulting force feedback F_i is displayed by a haptics interface, and corresponds to a simulated grasping task. The haptics interface allows us to manipulate the $x_i \rightarrow x_o$ and $F_i \leftarrow F_o$ transmission relationships in different ways to isolate the role of force and excursion mapping on function. Top diagrams (left to right) adapted from [13], [14], and [15].

Manuscript received 10 April 2023; revised 26 June 2023; accepted 11 July 2023. Date of publication 20 July 2023; date of current version 28 July 2023. This work was supported in part by the University of California at Berkeley. The work of Michael E. Abbott was supported by the National Science Foundation Graduate Research Fellowship Program under Award DGE 1752814. *(Corresponding author: Michael E. Abbott.)*

This work involved human subjects or animals in its research. Approval of all ethical and experimental procedures and protocols was granted by the University of California at Berkeley under Protocol No. 2019-05-12178.

The authors are with the Mechanical Engineering Department, University of California at Berkeley, Berkeley, CA 94720 USA (e-mail: michael_abbott@berkeley.edu; hstuart@berkeley.edu).

This article has supplementary downloadable material available at https://doi.org/10.1109/TNSRE.2023.3297549, provided by the authors.

Digital Object Identifier 10.1109/TNSRE.2023.3297549

Extended Physiological Proprioception (EPP) by D.C. Simpson in [16], one of the reasons often cited as crucial to body-powered functional performance and continued use [17]. However, users of BP prostheses still express a lack of satisfaction with their devices [3]. A major component is the high forces required from the user to operate the prosthesis, which leads to dissatisfaction [7] as well as worsened force control and fatigue concerns [18], [19].

Recent works show that body-powered (BP) prosthesis users perform better across a number of metrics than their myoelectric counterparts, including quicker and more frequent use [6], more accurate aperture sizing [20], and clinical task completion time [21]. However, these studies are typically performed at the device level, comparing user performance across entirely different prostheses. The design decisions underlying each prosthesis tested, such as contact friction and actuation method, all influence the resulting overall performance, making it difficult to extract specific reasons behind observed differences. One primary reason postulated for the functional improvement in BP prostheses is the inherent sensation of position and force enabled. A number of prior works elucidate the role of force feedback in BP prostheses for specialized functions, like stiffness discrimination, by comparing performance with the binary presence or absence of haptic force feedback, such as [17], [22]. These studies do not incrementally vary the magnitude of the feedback.

In a previous study, we systematically varied the degree of force feedback experienced during simulated grasping trials for the first time [23]; we did not include any evaluation of excursion. The present work represents an evolution of [23] by varying both input excursion (cable travel) and force to isolate their independent and coupled roles in accomplishing an experimental grasping task. Although the physical test bed is similar to that in [23], we collect a new and expanded set of human subjects data under new test conditions, both validating the prior findings and yielding entirely new insights. By better understanding the underlying tradeoffs in different force and position mappings, we aim to improve the state of the art in body-powered transmission design for novel prostheses.

A. Overview

We present results from a series of grasp and lift tasks under a variety of force and position mappings using a custom prosthesis emulator, visualized in Fig. 1. In Section II, we detail the components of the prosthesis emulator test bed, task protocol, performance metrics, and analytical methods used. Results presented in Section III show the effect of varying force and position inputs on both functional outcome measures and qualitative perceptions of the device, discussed further in IV. Section V presents conclusions and future work.

II. Experimental Methods

A. Test Bed

To evaluate the role of shoulder force and cable excursion in the operation of body-powered prostheses, we replicate the required loads and motions with a custom emulator, detailed in [23]. A revised version of the test bed, shown in Fig. 2,

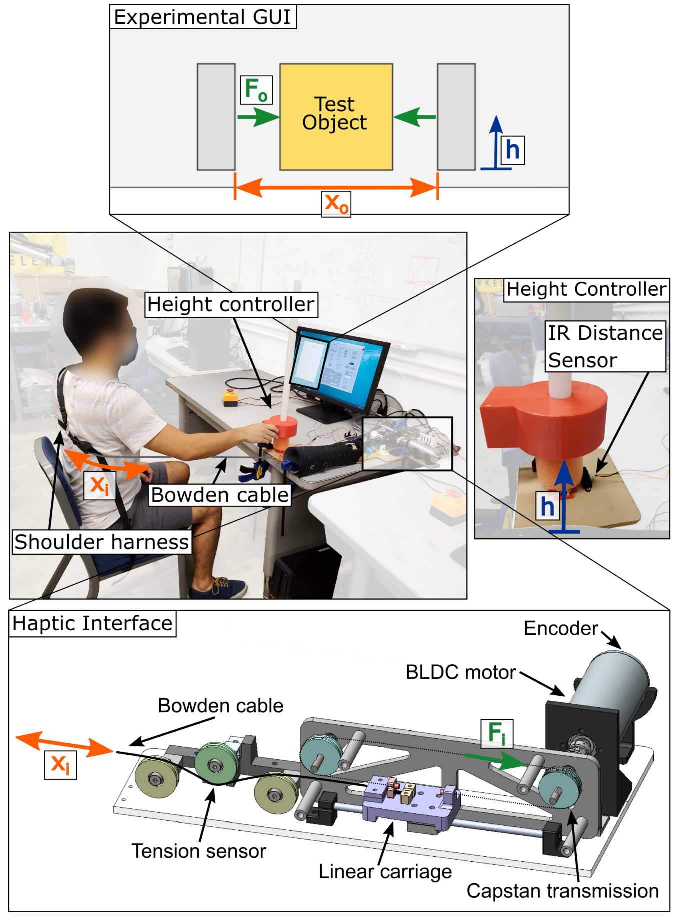

Fig. 2. System overview of the prosthesis emulator test bed. Motion of the user's contralateral shoulder x_i controls the aperture x_o and grasp force F_o of a virtual gripper in an Experimental GUI, while motion of the height controller sets its height h. A custom haptic interface, pictured in a cross-sectional view at the bottom, measures cable excursion and outputs cable forces F_i back to the user. Adapted from [23].

comprises four subsystems: a figure-of-nine shoulder harness, a height controller, a desktop haptic interface, and a virtual grasping environment visualized in an experimental Graphical User Interface (GUI). A supplemental video demonstrates integrated operation of the test bed.

The haptic interface is an impedance-style device which relates user input motion x_i to input forces F_i. It translates the motion and forces of the user's shoulder to those of a virtual gripper through a Bowden cable connecting the harness and haptic interface. A linear carriage constrains the cable's excursion to a single degree of freedom, and a capstan transmission ties this linear motion to the shaft of a brushless DC (BLDC) motor (Maxon, EC-i 52) in a stiff, low-inertia manner free of backlash. An encoder fixed to the motor shaft (Maxon, ENC 16 EASY) measures the motion of the shaft (and therefore shoulder excursion x_i). We convert x_i to a commanded virtual gripper aperture x_o by scaling it by a position mapping gain K_p such that

$$x_o = x_{o,0} - K_p x_i \tag{1}$$

where $x_{o,0}$ is the initial aperture. By defining the width of the test object w and a contact stiffness k_c, we estimate the applied grasp force F_o needed to reach the commanded aperture:

$$F_o = \begin{cases} 0 & x_o \geq w \\ k_c \dfrac{(w - x_o)}{2} & x_o < w \end{cases} \quad (2)$$

assuming the gripper height is aligned with the height of the object ($F_o = 0$ otherwise). We scale F_o by a force mapping gain K_f to determine the desired feedback force $F_{i,des}$ to display to the user such that $F_{i,des} = K_f F_o$.

The height controller sets the height, h, of the virtual gripper and consists of an IR distance sensor and 3D-printed handhold. A one-dimensional dynamic model governs the motion of the test object based on the current grasp force and specified contact and object properties, such as friction coefficient, mass, and size. Motion of the test object is limited to the vertical direction and defined by the following dynamic model:

$$\ddot{h}_{object} = \begin{cases} \ddot{h}_{gripper} & \text{no slip} \\ \dfrac{1}{m}(2\mu F_o) - g & \text{slip} \end{cases} \quad (3)$$

where g is the acceleration due to gravity, m is the object mass, and slip is defined as occurring when the grasp force is not high enough to produce sufficient friction force, with a maximum magnitude of $\mu F_{o,i}$, to resist the inertial and gravity loads on the test object.

The GUI, pictured at the top of Fig. 2, displays the height of the gripper $h_{gripper}$ and the test object h_{object} as well as the grasp aperture x_o. The change in aperture, related to x_i and the selected value of K_p as in Eq. 1, is visually displayed to user, but no visual indication is provided for sufficient grasp force generation beyond the slip of the object in the grasp and the "breaking" of the object when excessive grasp force is applied. For a "break," the test object changes color from yellow to red when the grasp force exceeds four times the minimum force to prevent slip.

The motor produces a linear cable force F_i back to the user through the same transmission and harness. An inline tension sensor provides the feedback signal for a PI controller to drive the actual force F_i to the desired cable force $F_{i,des}$ plus a constant offset of 6 N to maintain tension in the cable. The controller features anti-windup via back-calculation and is implemented along with data acquisition via LabVIEW. With this setup, we can flexibly manipulate the relationships between the forces and motions experienced by the user at their shoulder by changing the value of either K_f or K_p. An operational block diagram of the test bed is shown in Fig. 3.

B. Study Procedure

Data represent a total of 15 non-amputee participants (5 female, 10 male) with normative upper limb function. Participant ages range between 18 and 68 with a mean of 28.4 years old. All experimental procedures are approved by the University of California, Berkeley Institutional Review Board (protocol #2019-05-12178, approved 10/16/2019), and informed consent was received from all participants prior to experimentation.

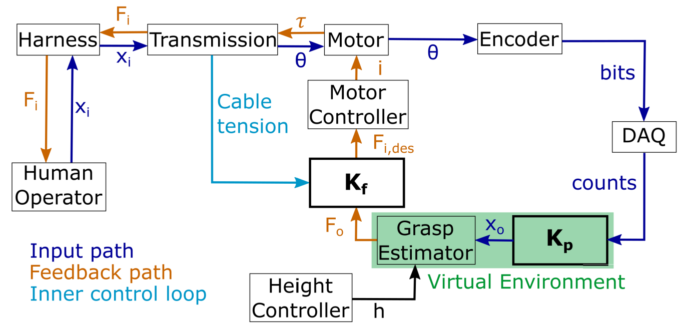

Fig. 3. Block diagram for operation of the experimental test bed. Key experimental parameters of force mapping gain K_f and position mapping gain K_p are marked in bold. Adapted from [23].

1) Fitting and Initialization: Participants perform the experiment seated in a chair facing a desk where the test bed is mounted and the task GUI is displayed. They don the figure-of-nine shoulder harness which is then adjusted by the experimenter to ensure a proper fit with the participant's particular body morphology. Once the system is homed and initialized, the carriage position is locked, and the participant is asked to adjust their seat position such that there is light pretension (<5 N) on the cable with their backs against the chair backrest and their shoulders adducted.

2) Trial Protocol: Each trial consists of a grasp, lift, and hold task modeled after normative grasp studies [24]. For all trials, we assign m as 1.5 kg, w as 5 cm, μ as 0.7, and k_c as 5 kN/m; the minimum F_o is 10.5 N for lift-off. The subject closes the gripper using the shoulder harness until they believe they have applied sufficient grasp force. They then raise the height controller to lift the gripper and object a minimum of 15 cm, marked in the GUI by a dashed line, which they attempt to maintain for at least 3 seconds. Finally, the subject releases the object, through relaxing the shoulder harness, and returns both the object and gripper to the base level to conclude the trial. Visual indicators in the GUI mark when the object has been lifted to a sufficient height and held for a sufficient amount of time.

3) Experimental Conditions: We divide the testing into three testing blocks of different experimental conditions: *Force*, *Position*, and *Combined*. In the *Force* block, we isolate the role of force feedback by varying the force mapping gain $K_f = [0.5, 0.75, 1, 1.5, 2]$ while keeping the position mapping gain constant at $K_p = 1$. In the *Position* block, we maintain a constant $K_f = 1$ value and vary $K_p = [2, 1.5, 1, 0.75, 0.5]$ to evaluate the role of shoulder movement. Varying K_f and K_p in isolation allows for the independent study of each variable. In the *Combined* block, we vary both K_f and K_p simultaneously in a manner which emulates passive transmissions with more realistic design constraints, where force and position mappings are inversely related. Akin to changing the length of the input lever arm – like the class III lever in most BP prehensors – we set K_f and K_p^{-1} equal to the transmission ratio TR for each tested condition. Because of this inverse force-motion tradeoff, we plot Position block results against K_p^{-1}.

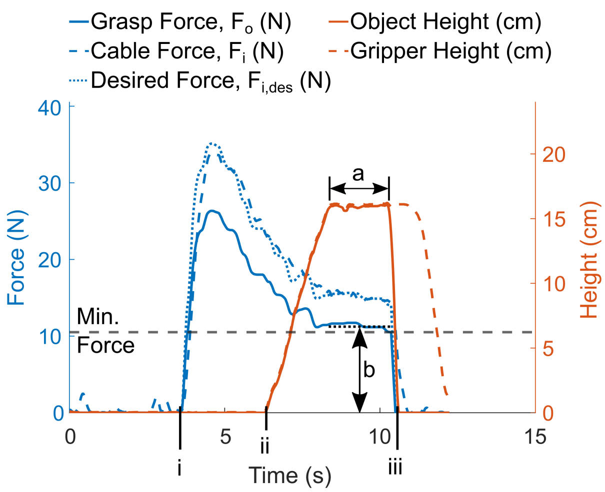

Fig. 4. Sample force and height data measured over time from a single grasping trial with a force mapping gain $K_f = 0.75$. Roman numerals mark key events during the trial: i) first virtual gripper contact with test object, ii) initiation of lift of the test object, and iii) release and descent of the test object. Letters denote key trial metrics and parameters: a) hold region, b) mean grasp force (averaged over the hold region). The minimum grasp force to prevent slip is marked as a grey dashed line.

For each testing block, participants complete 10 trials at 5 different system configurations whose order is pseudorandomized with a Fisher-Yates shuffle. Prior to each new system configuration, participants are allowed practice trials until they signal to the experimenter that they are ready to begin. Both functional and qualitative measurements are taken in order to establish performance metrics.

C. Measurements and Performance Metrics

1) Functional Metrics: Force, height, and excursion data are recorded at a rate of 60 Hz throughout each trial. Data collected from a representative trial are plotted in Fig. 4 where $K_f = 0.75$ and $K_p = 1$. At time i), the participant makes first contact with the object then increases their applied grasp force, thus experiencing the resulting cable force. They begin to lift the gripper and object at time ii) until they reach a height plateau above the minimum height of 15 cm. At time iii), grasp force reduces and object falls to the ground state.

We portion the data into grasp phases using local linear regressions of a sliding window of 7 points. We define the phases and transitions with the following criteria:

- *Grasp loading*: grasp force slope positive and greater than 5% of maximum grasp force measured.
- *Lift-off*: gripper height slope positive and greater than 5% of maximum gripper height reached.
- *Hold*: object height slope less than 1% of maximum object height reached and object height above threshold.
- *Release*: object height slope negative with absolute value greater than 5% of maximum object height reached.

If no plateau is reached above the height threshold, we instead use the points where the object height crosses the minimum lift height threshold to define the holding phase.

We then define and calculate a number of grasp performance metrics from the trial data:

- *Accidental drop*: hold phase duration less than 3 seconds.[1]
- *Mean grasp force*: average F_o during the hold phase.
- *Within-trial (WT) grasp force MAD*: mean absolute deviation (MAD) of F_o during the hold phase.
- *Between-trial (BT) grasp force MAD*: MAD of the mean grasp forces between trials under the same system configuration.

We also calculate the mean cable force F_i and excursion x_i during the hold phase to evaluate the loads and motions experienced by participants under the different system configurations in order to report test bed performance.

2) Qualitative Metrics: At the end of each set of 10 trials per system configuration, participants are asked a brief series of three qualitative questions to gauge their perceived experiences. The first two are Likert-style questions where subjects are asked to rate their level of agreement or disagreement with given statements regarding ease of use (*Easy*) and comfort (*Comfortable*) on a six-point forced-choice scale. The third and final question asks for a rating of their perceived exertion during the tasks in the given configuration based on the Borg CR10 Scale [25] to establish a *Borg CR10 Score*, where a score of 0 relates to a rating of "No exertion at all" and a score of 10 a rating of "Extremely strong (maximal exertion)". Following the completion of each testing block, subjects are asked for general *sentiments*, i.e. preferences and dislikes between the experienced system configurations, which are subsequently coded as "Prefer", "Neutral", or "Dislike" for later analysis. Survey details can be found in Appendix A.

D. Statistical Analysis

All statistical modeling is performed with R v4.2.2. We use mixed model regression to analyze the role of position and force mappings on the selected performance metrics. We treat mapping gains as an ordinal predictor variable to enable post-hoc between-level comparisons and include configuration order (CO, the order in which transmission conditions are experienced) and trial number (T, the order in the set of grasping attempts per transmission condition) as covariates to control for potential learning or fatigue effects. Regression is done with polynomial contrasts and fits a fourth-order polynomial model (for an ordinal variable of 5 levels) between the predictor and outcome variables of interest, where each coefficient is noted as $.L$, $.Q$, $.C$, and^4, respectively. Model selection is performed for model parsimony using Likelihood Ratio Tests (LRTs) to identify the presence of autoregressive effects, interaction effects, and within-subject correlative effects.

For continuous data – mean grasp force, WT grasp force MAD, and BT grasp force MAD – we use linear mixed models (LMMs) with the "nlme" package [26]. A first-order autoregressive (AR(1)) correlation structure is imposed to account for observed autocorrelation of lag 1. We include the maximal random effect structure (slope and intercept) for participant ID to account for significant within-subject correlation, as recommended in [27]. Outcome variables for mean grasp force and

[1] A 5% buffer with respect to duration is allowed to limit the number of false positives by accounting for slight inaccuracies in hold phase estimation.

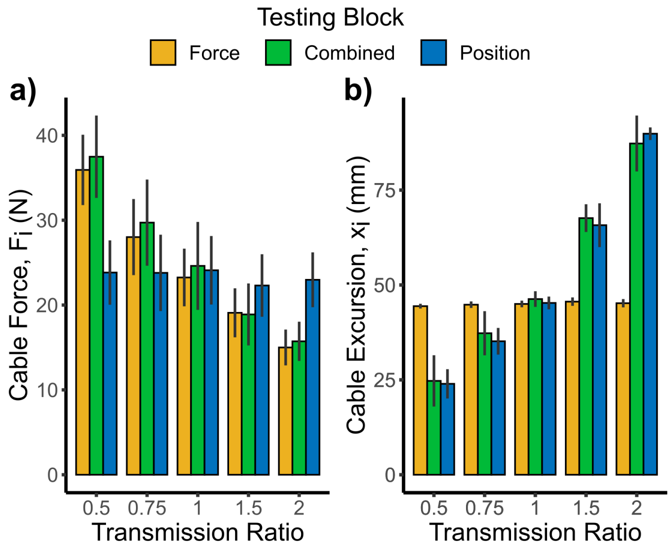

Fig. 5. Mean cable force (a) and excursion (b) across all trials and participants. Error bars denote standard deviation in force or excursion at each transmission ratio configuration. For Force and Position results, "Transmission Ratio" refers to the force or inverse position mapping gains used for that transmission ratio, e.g., $TR = 0.75$ equates to $K_f = 0.75$ and $K_p^{-1} = 1$ for Force data and $K_p^{-1} = 0.75$ and $K_f = 1$ for Position data and $K_f = K_p^{-1} = 0.75$ for Combined data.

WT force MAD are log-transformed prior to model fitting to normalize residuals in mean grasp force and BT grasp force MAD due to observed heteroskedasticity. For non-continuous outcome measures – accidental drop rate and survey results – we use generalized regression methods. We apply mixed-effect logistic regression to analyze the binary outcome of accidental drops with the "lme4" package [28]. Cumulative link mixed models (CLMM) are employed to analyze all survey data with the "ordinal" package [29] to avoid biases inherent to metric models and Likert-style data [30].

We then calculate estimated marginal means (EMMs) across factor levels of force gain, position gain, or transmission ratio for all outcome variable models with the "emmeans" package [31]. Post-hoc pairwise comparisons are performed with Tukey's Honest Significant Difference Test.

III. Results

A. User Inputs Across Testing Blocks

Measured cable forces and excursions are reported in Figure 5. As expected, participants in the Force testing block experience decreasing cable forces in (a), from 35.9 to 15.0 N, with increasing K_f while keeping cable excursion constant in (b). In the Position block, participants experience relatively constant cable forces in (a) and increasing cable excursions (26.4 to 87.8 mm) with decreasing K_p (denoted here as increasing transmission ratio). In the Combined block, participants simultaneously experience increasing force mapping gains in (a) and decreasing position mapping gains in (b), resulting in similar cable force levels to those in the Force block and similar cable excursions to those in the Position block. These variations in motion and force inputs from participants indicate that users adapt to the different transmission configurations to achieve successful grasps rather than targeting a specific body position or muscle output across all configurations.

B. Force Block

1) Functional Outcomes: As seen in Figure 6(a), participants exhibit a negative quadratic effect for mean grasp force with increasing force mapping gain ($K_f.Q$: $b = -0.226$, $p = 5.18e-4$), which means that subject apply lower output grasp forces for higher experienced shoulder forces. They apply the lowest grasp forces at low values of K_f (14.5 N and 40% safety margin over slip with $K_f = 0.5$) and highest forces at moderately high to high values of K_f (19.0 N and 81% safety margin over slip with $K_f = 1.5$). We also observe a positive interaction with configuration order ($K_f.Q : CO$: $b = 0.0517$, $p = 0.00884$), suggesting a diminished effect of force gain as the experiment progressed.

While grasping the object, Figure 6(b) shows that participants exhibit a positive cubic effect with WT force MAD ($K_f.C$: $b = 0.414$, $p = 0.0439$), with grasp forces varying more (i.e. less steady) at higher force gains and lower experienced shoulder forces. A negative quartic interaction with configuration order ($K_f.\hat{}4 : CO$: $b = -0.0961$, $p = 0.0480$) and negative quadratic and cubic interactions with trial number ($K_f.Q : T$: $b = -0.0680$, $p = 6.19e-4$, $K_f.C$: $b = -0.0386$, $p = 0.0480$) suggest a learning effect where applied grasps become steadier with practice. However, WT force MAD marginal means vary within a small range (0.516 N to 0.674 N) with only one significant pairwise difference; variations in WT grasp force steadiness across K_f therefore appear functionally inconsequential.

Between trials, Figure 6(c), participant grasp force is more variable for lower experienced input forces and higher values of K_f with a positive linear effect ($K_f.L$: $b = 0.625$, $p = 0.0293$) and negative cubic and quartic effects ($K_f.C$: $b = -0.637$, $p = 0.00978$, $K_f.\hat{}4$: $b = -0.643$, $p = 0.00921$) for BT force MAD with force mapping gain. A K_f value of 1.5 led to significantly more variable forces with a marginal mean BT force MAD of 4.18 N. From this, we see that experiencing higher shoulder forces leads to more consistent force application grasp to grasp. No observed interactions or significant covariates suggest relatively small effects, if any, from learning or fatigue.

Accidental drop rate, Figure 6(d) shows that increasing K_f and decreasing the experienced user force input results in a significant negative linear effect ($K_f.L$: $b = -1.16$, $p = 1.06e-4$), decreasing from 25.4% at $K_f = 0.5$ to less than 8.6% for $K_f > 1$. Pairwise comparisons indicate improvements in drop rate up to a gain of 1 (17.2 N of required input force), but little improvement for higher gains. This trend makes sense given that subjects apply larger grasp force safety margins at higher force gains, as in (a).

2) Qualitative Outcomes: Participants generally express more positive attitudes about system configurations with low user forces and high force gains, shown in Fig. 7. In (a), they find the system easier to use ($K_f.L$: $b = 3.05$, $p = 1.89e-05$) and (b) more comfortable ($K_f.L$: $b = 3.58$, $p = 0.00147$). At the same time, (c) they perceive less exertion ($K_f.L$: $b = -4.78$, $p = 3.39e-09$) when applying lower shoulder

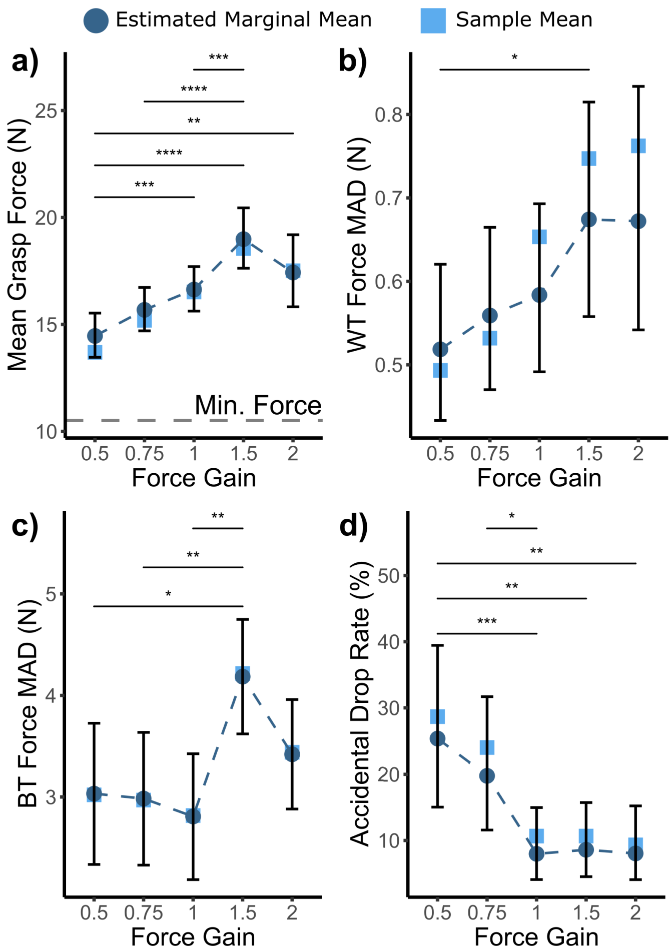

Fig. 6. Summary of grasp performance metrics (a)-(d) during the Force block. The grey dashed line in (a) marks the minimum grasp force to prevent slip. Dark blue points represent model-based estimated marginal means, light blue squares represent sample means, and error bars denote the standard error of the estimated marginal means. Asterisks denote significant pairwise comparisons of estimated marginal means (* $= p < 0.05$, ** $= p < 0.01$, *** $= p < 0.001$, **** $= p < 0.0001$).

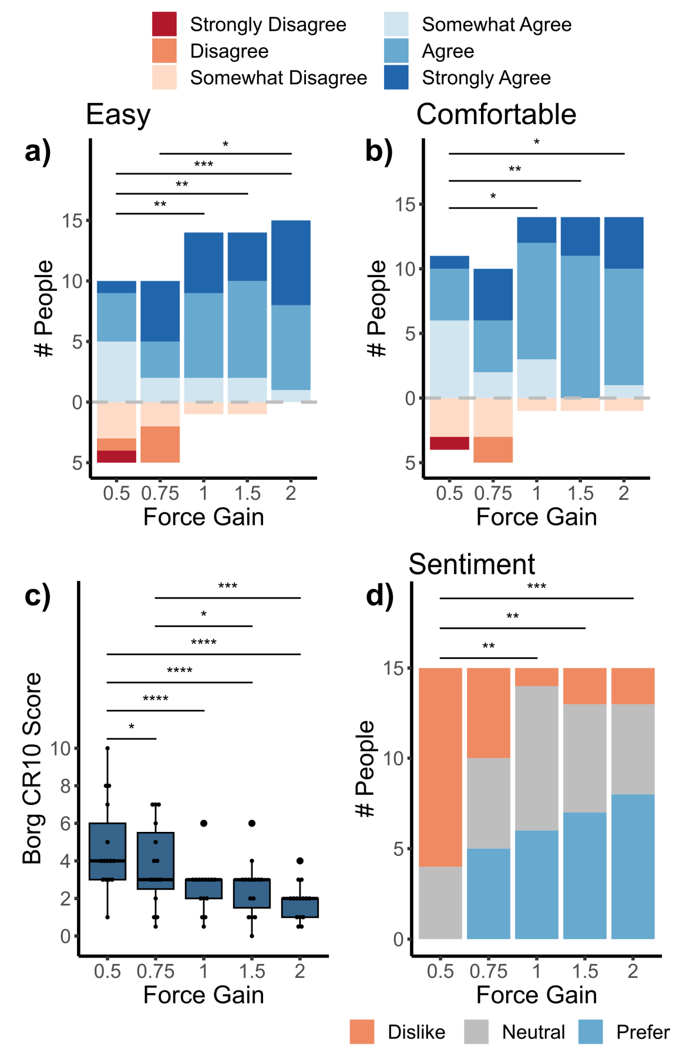

Fig. 7. Summary of qualitative results (a)-(d) during the Force block. In the boxplot, the dividing line marks the median, the edges denote the first and third quartiles, whiskers are limited to lengths equal to 1.5 times the IQR, and outliers are marked as points. Asterisks denote significant pairwise comparisons of estimated marginal means (* $= p < 0.05$, ** $=$ $p < 0.01$, *** $= p < 0.001$, **** $= p < 0.0001$).

forces with higher values of K_f. Median scores decrease from "4 - Moderately Strong" at the highest experienced shoulder forces to "2 - Weak" at the lowest forces, though some participants report scores as high as "10 - Extremely strong (maximal exertion)" at $K_f = 0.5$. It is therefore unsurprising that (d) subjects report higher force gains to be more preferable ($K_f.L$: $b = 2.30$, $p = 5.93e - 05$, $K_f.Q$: $b = -1.20$, $p = 0.0227$).

Pairwise comparisons highlight a particular dislike for force gain of 0.5 (average cable force of 35.9 N) across all qualitative measures, and a dislike under the categories of force gain of 0.75 (average force of 28.0 N) for (a) ease and (c) exertion. No significant effects with respect to configuration order or two-way interactions are observed, suggesting little perceived learning benefits or fatigue-related deficiencies during the course of the testing block.

C. Position Block

1) Functional Outcomes: From results presented in Fig. 8, we observe a negative quadratic effect with inverse position gain ($K_p^{-1}.Q$: $b = -0.0716$, $p = 0.0456$) for mean grasp force (a), suggesting decreased grasp forces at small and large shoulder excursions. The mean grasp force decreases from ≥ 17.3 N for $K_p^{-1} \leq 1$ to 15.4 N at $K_p^{-1} = 2$. We also see a reduction in the effect of position gain with a negative linear interaction with trial number ($K_p^{-1}.Q : T$: $b = -0.0101$, $p = 0.0483$). Pairwise comparisons show no significant differences between selected gains due to small range (1.9 N) and relatively large EMM confidence intervals.

Varying cable excursions appears to have limited effect on the magnitude of force variability as well, both in terms of WT (b) and BT force MAD (c). Participants show a positive cubic effect ($K_p^{-1}.C$: $b = 0.380$, $p = 9.83e - 4$) and negative cubic interaction with trial number ($K_p^{-1}.C : T$: $b = -0.0558$, $p = 0.00215$) for WT force MAD. For BT force MAD, we observe a negative linear effect with position gain ($K_p^{-1}.L$: $b = -2.04$, $p = 0.0180$) and a negative effect

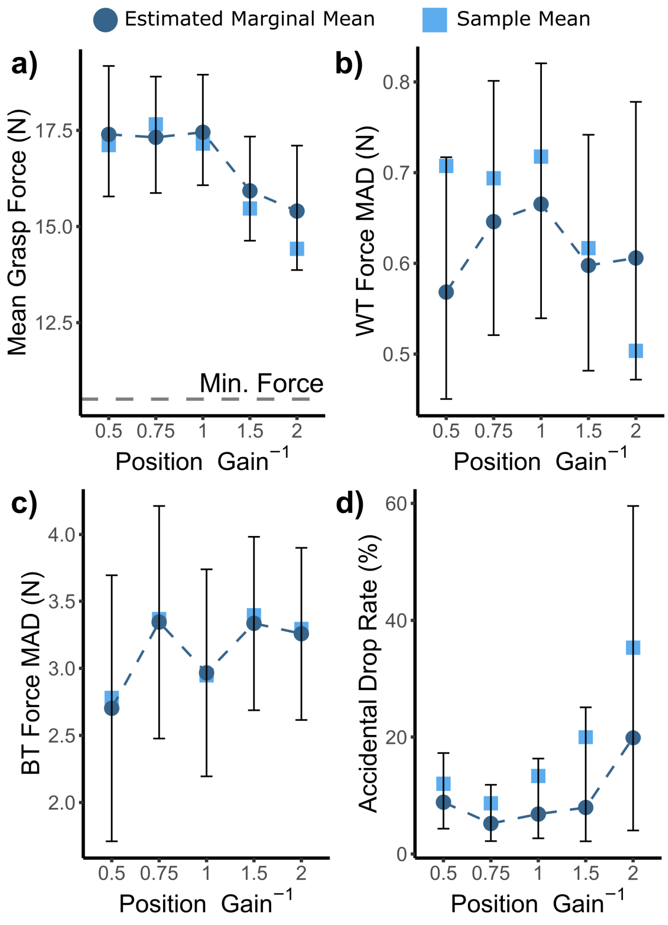

Fig. 8. Summary of grasp performance metrics (a)-(d) during the Position block. The grey dashed line in (a) marks the minimum grasp force to prevent slip. Dark blue points represent model-based estimated marginal means, light blue squares represent sample means, and error bars denote the standard error of the estimated marginal means. Asterisks denote significant pairwise comparisons of estimated marginal means (* $= p < 0.05$, ** $= p < 0.01$, *** $= p < 0.001$, **** $= p < 0.0001$).

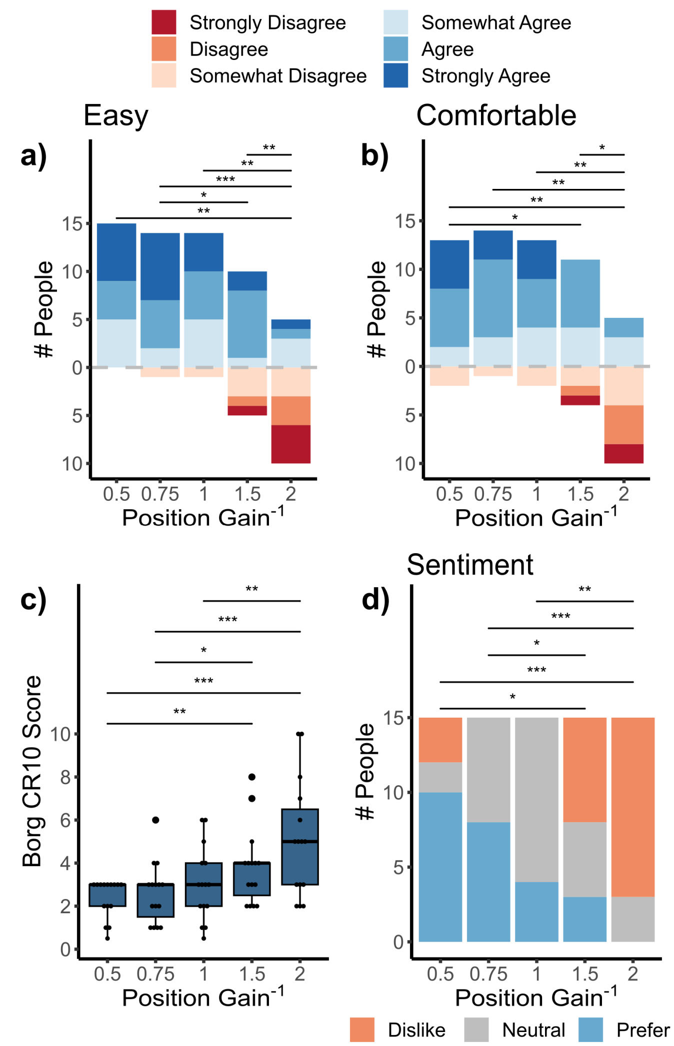

Fig. 9. Summary of qualitative results (a)-(d) during the Position block. In the boxplot, the dividing line marks the median, the edges denote the first and third quartiles, whiskers are limited to lengths equal to 1.5 times the IQR, and outliers are marked as points. Asterisks denote significant pairwise comparisons of estimated marginal means (* $= p < 0.05$, ** $= p < 0.01$, *** $= p < 0.001$, **** $= p < 0.0001$).

with trial (T: $b = -0.122$, $p = 0.0353$), as well as a positive linear interaction between position gain and configuration order ($K_p^{-1}.L : CO$: $b = 0.833$, $p = 5.57e-4$), negative cubic interaction with trial number ($K_p^{-1}.C : T$: $b = -0.204$, $p = 2.82e-4$), and positive interaction between configuration order and trial ($CO : T$: $b = 0.0390$, $p = 0.0260$). However, both variability measures show little effect from changing position gain, with no significant pairwise comparisons and small ranges (0.10 N for WT force MAD and between 0.64 N for BT force MAD). These results suggest little practical consequence despite significant observed trends.

Accidental drop rate (d) exhibits a significant positive quadratic effect ($K_p^{-1}.Q$: $b = 0.836$, $p = 0.00483$) with respect to position gain, with a distinctly higher drop rate for the largest excursion $K_p^{-1} = 2$ of 19.9% (mean excursion of 87.8 mm) compared to drop rates less than 8.9% for $K_p^{-1} \leq 1.5$ (mean excursions less than 68.5 mm). We observe no significant effect of configuration order or trial nor interactions, suggesting small if any fatigue or practice effects. Pairwise comparisons show no significant differences in drop rate between position gains, likely due to the large confidence interval for high K_p^{-1} values.

2) Qualitative Outcomes: Participants generally express positivity about system configurations with low ranges of motion and low K_p^{-1} values, as shown in Fig. 9. They find the system less comfortable (b) ($K_f.L$: $b = -5.35$, $p = 0.000367$, $K_f.Q$: $b = -1.998$, $p = 0.00748$) and more exertive (c) ($K_f.L$: $b = 4.24$, $p = 1.39e-05$) with increasing K_p^{-1}. Median Borg CR10 scores increase from "3 - Moderate" for $K_p^{-1} \leq 1$ to "5 - Strong" for $K_p^{-1} = 2$. We observe similar negative trends in interactions with configuration order in terms of (a) ease of use ($K_f.L : CO$: $b = -2.29$, $p = 0.00848$, $K_f.Q : CO$: $b = -2.19$, $p = 0.0147$) and (d) preference ($K_f.L : CO$: $b = -1.78$, $p = 0.030$), suggesting the detrimental effect of increasing shoulder excursion worsens over time, possibly due to fatigue. Similar to Force block results, pairwise comparisons between marginal means reveal a significant decrease in qualitative outcomes for K_p^{-1} values

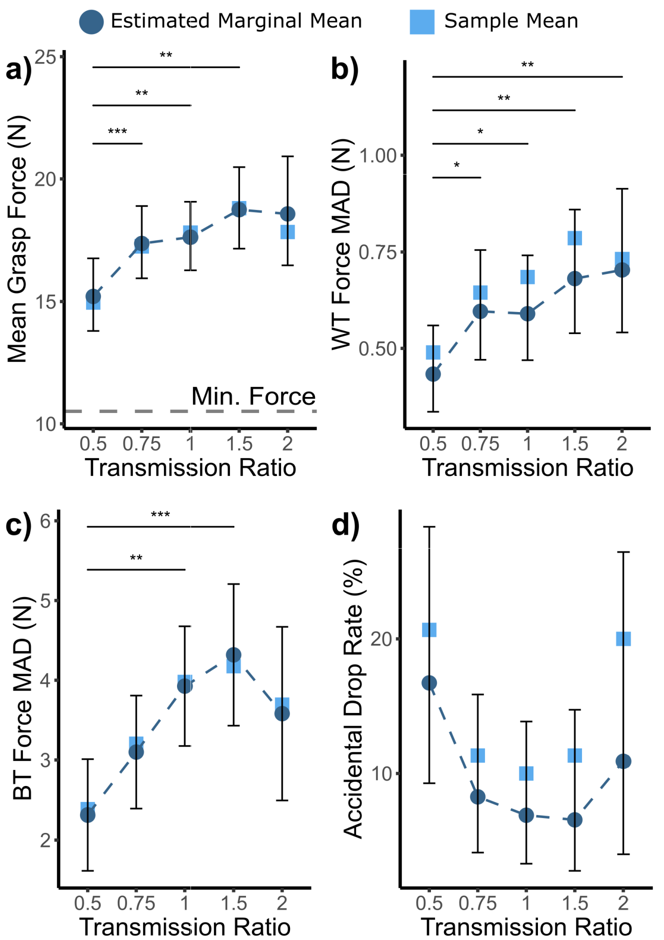

Fig. 10. Summary of grasp performance metrics (a)-(d) during the Combined block. The grey dashed line in (a) marks the minimum grasp force to prevent slip. Dark blue points represent model-based estimated marginal means, light blue squares represent sample means, and error bars denote the standard error of the estimated marginal means. Asterisks represent significant pairwise comparisons of estimated marginal means (* $= p < 0.05$, ** $= p < 0.01$, *** $= p < 0.001$, **** $= p < 0.0001$).

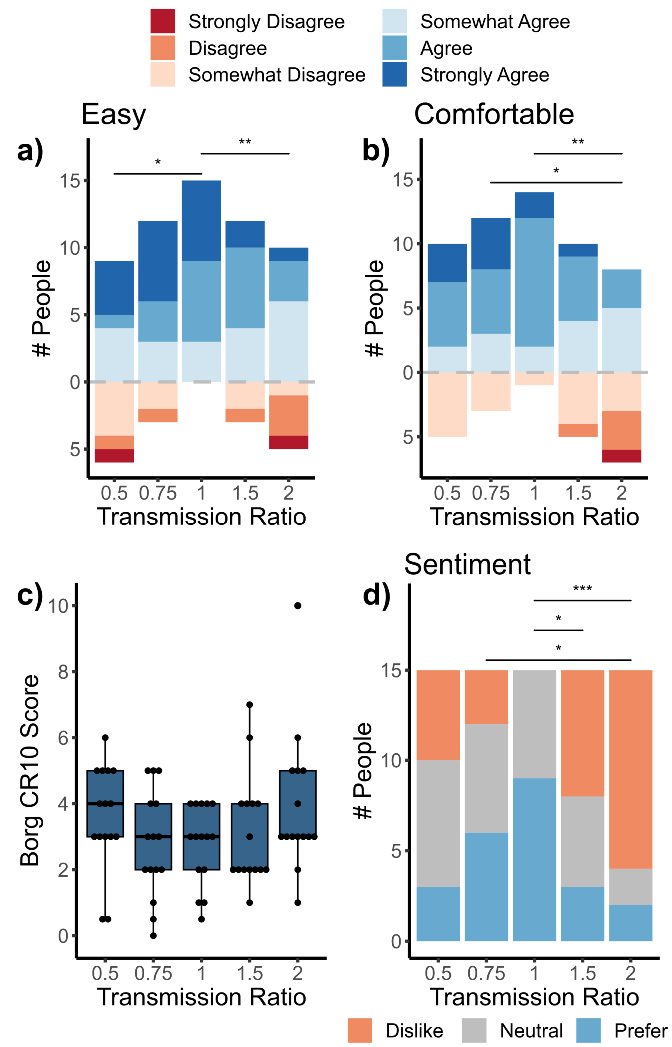

Fig. 11. Summary of qualitative results (a)-(d) during the Combined block. In the boxplot, the dividing line marks the median, the edges denote the first and third quartiles, whiskers are limited to lengths equal to 1.5 times the IQR, and outliers are marked as points. Asterisks represent significant pairwise comparisons of estimated marginal means (* $= p < 0.05$, ** $= p < 0.01$, *** $= p < 0.001$, **** $= p < 0.0001$).

of 1.5 and 2 and average cable excursions of 65.8 mm and 89.9 mm, respectively. No other significant effects are observed, suggesting little perceived learning benefits.

D. Combined Block

1) Functional Outcomes: As seen in Figure 10(a), participants apply increasing grasp forces with increasing transmission ratio values with positive observed linear and quadratic effects ($TR.L$: $b = 0.273$, $p = 0.00169$, $TR.Q$: $b = 0.243$, $p = 0.00120$). They apply the lowest force at low TR values (15.5 N at $TR = 0.5$) and the highest forces at the highest TR values (19.1 N at $TR = 1.5$, 18.9 N at $TR = 2$). A negative quadratic interaction with configuration order ($TR.Q : CO$: $b = -0.101$, $p = 2.36e-5$) implies a smaller effect of transmission ratio as the experiments progress.

Grasp force variability also increases with transmission ratio, with a linear effect with transmission ratio for (b) WT force MAD ($TR.L$: $b = 0.348$, $p = 0.00119$) and positive linear and quadratic effects with transmission ratio for (c) BT force MAD ($TR.L$: $b = 2.79$, $p = 0.00176$, $TR.Q$: $b = 2.44$, $p = 0.00254$). WT force MAD increases from a low of 0.546N at $TR = 0.5$ to a high of 0.886 N at $TR = 2$. BT force MAD starts at a low of 2.31 N at $TR = 0.5$, increases to 4.32 N at $TR = 1.5$, and then decreases slightly to 3.58 N at $TR = 2$. The effect of practice may decrease variation with observed negative linear and quadratic interactions between transmission ratio and configuration order ($TR.L : CO$: $b = -0.533$, $p = 0.048$; $TR.Q : CO$: $b = -1.12$, $p = 1.23e-5$).

In (d), participants show higher drop rate EMMs at low and high transmission ratio values, 16.7% and 10.9%, respectively. Supporting this, we see a significant positive quadratic effect between accidental drop rate and transmission ratio ($K_f.Q$: $b = 0.764$, $p = 0.00467$) as well as no significant effect of covariates or their interactions, signifying no evidence of fatigue or learning effects in task success over time. However, no significant differences in drop rate between transmission ratios are found from pairwise comparisons, likely due to the large confidence intervals for low and high TR values as in the Position block.

2) Qualitative Outcomes: In the Combined block, participants prefer moderate transmission ratios that balance excursion and force. Poorer qualitative outcomes occur at both low and high transmission ratio configurations, as seen in Fig. 11. This is further supported by significant quadratic effects which reveal detrimental effects of extreme transmission ratios in terms of (a) ease of use ($TR.Q$: $b = -2.85$, $p = 4.8e-05$), (b) comfort during operation ($TR.Q$: $b = -2.03$, $p = 0.00123$), (c) perceived exertion ($TR.Q$: $b = 2.05$, $p = 0.000388$), and (d) preference ($TR.Q$: $b = -1.96$, $p = 0.000377$). Comfort ($TR.L$: $b = -2.44$, $p = 0.0115$) and preference ($TR.L$: $b = -1.39$, $p = 0.0105$) also show negative linear effects with increasing transmission ratio, suggesting that high transmission ratios – larger ranges of motion with lower required input forces – are less comfortable and less preferred than lower ratios. No significant effects with respect to configuration order or two-way interactions are observed. Pairwise comparisons show positive attitudes for a transmission ratio of 1 in terms of ease, comfort, and sentiment, but insignificant differences in perceived exertion scores between transmission ratio configurations despite changing force and excursion demands.

IV. Discussion

A. Grasp Test Results

When comparing results across the three different test blocks, the mean grasp force and force MAD trends from the force block resemble those observed in the combined case in both shape and magnitude, with position block results exhibiting smaller magnitudes and different trends. This suggests that for typical passive mechanical transmissions, where force and excursion are traded off, it is primarily the change in force gain which drives people's abilities to regulate grasp force. The accidental drop rate increases both with increasing shoulder force (i.e. low K_f in the Force block) and with increasing required excursion (i.e. high K_p^{-1}), trends seen in the combined testing block as well for low and high transmission ratios. It seems that both force and excursion independently contribute in opposition to higher drop rates.

The low WT grasp force MAD values, less than 0.75 N across all testing blocks, indicate that grasp forces remain relatively steady once a grasp has been secured. This combined with the substantially larger BT grasp force MAD values (2.5 - 4 N) suggest that accidental drops occur due to improperly set target grasp forces prior to lift rather than inappropriate force adjustments during the grasp. This feedforward uncertainty seen in higher BT MAD values could also explain the increase in mean grasp forces for the force and combined block results; participants increase their safety margin over slip in the presence of uncertain grasp conditions, as has been observed in normative grasping studies [32], [33].

Across all qualitative measures, participants show a preference towards lower input forces (high K_f) and excursions (low K_p^{-1}) in the Force and Position blocks, respectively. These effects appear to contribute in an additive manner, resulting in the parabolic shapes for the Combined block results which favor the moderate transmission ratios. The discomfort for high forces is not entirely offset by the benefits of small excursions, nor is the negativity towards large excursions offset by smaller required forces.

B. Relevance to Body-Powered Device Design

Based on the isolated testing done during the Force and Position testing blocks, designers of shoulder-driven body-powered devices should strive to limit both force and position gains to at or below 1 in their mechanisms. This relates to an average cable force of 24 N and average cable excursion of 45 mm in the present study, which is specific to this particular test bed and study configurations.Little benefit is derived from lowering force or position ratios further but significant negative differences appear with higher input forces or excursions. These numbers remain consistent even with the force-motion tradeoffs of the combined case. The largest number of individuals rated a moderate transmission ratio of 1:1 as preferred, with an average cable force of 25 N and average cable excursion of 46 mm, comparable to values in the isolated force and position blocks. Shoulder-driven prehensors on the market today provide transmission ratios of about 0.67:1 [34], which is close but slightly less that what our study found. This is likely to prioritize reducing the necessary range of motion which can be a limiting factor in BP prosthesis operation.

When studied independently, participants show a clear preference, both in terms of function and perception, for low forces and low ranges of motion when operating body-powered prostheses. While not feasible with traditional fixed transmissions which inherently involve force-position tradeoffs, future work could examine the possibility of variable transmissions in body-powered prostheses, such as those detailed in [35], [36], and [37]. Such a system has the potential to appropriately amplify output forces or positions based on user inputs and limit uncomfortable loads and postures from the user.

Across all 3 testing blocks, and especially for the Position block, we observe more pronounced differences in qualitative outcomes than those in functional outcomes. Participants demonstrate an ability to adapt to the changing force and positional demands in terms of their grasp performance but with varying levels of ease and comfort. This encourages continued research into the development and validation of self-perception metrics, as well as their inclusion alongside traditional clinical functional tests, for a holistic assessment of overall performance.

C. Limitations and Future Work

In analyzing these data, we find large confidence intervals in drop rate EMMs and mismatch between estimated and sample means, particularly for conditions which varied K_p. This is likely due to large differences in participant ranges of motion, which resulted in great difficulty for some in reaching the required excursion for high values of K_p^{-1} and accidental drop rates for those individuals equal to or greater than 80%. This would bias participant arithmetic means but be mitigated by the random slope and intercept given to each participant in the modeling process and following EMM, potentially explaining this discrepancy. Future work should additionally evaluate cable forces and excursions in relation to each individual's maximum voluntary contraction and range of motion to investigate whether the ratios or magnitudes of force and motion are the driving factors in evaluation measures.

During the experiment, participants can only gauge their performance with limited binary feedback of task success or failure. Though significant autocorrelation in all cases implies prior success or failure drives adaptation, it does not provide other factors present in real-world grasping such as weight perception. Following these results, future work should include grasping tasks which involve physical objects with realistic weights and contact conditions. This could also open further studies into new aspects of prosthetic grasping, such as the coordination between lift and grasp forces seen in normative grasping [24].

Future studies with a physical end-effector could elucidate further design considerations for BP devices. These could include manipulations occurring outside of the single plane used in this test bed, such as side or overhead reaches, as well as bimanual tasks. Such studies could also take into account other physical device considerations like the initial setting of the effective control cable length, which is not adjustable in the prosthesis emulator used in this work. The amount of excursion and force that can be feasibly generated would likely be affected by several of these factors, as discussed in [38], potentially leading to differing user preferences or performance.

In this work, participants also only interact with one object (i.e. constant size, mass, and stiffness), so some findings may not generalize to other real-world objects. For example, a small object might lead towards a preference for low transmission ratio systems which amplify gripper motion (at the expense of grasp force), while a heavy object may lead to preferences for high transmission ratio systems which amplify grasp force (at the expense of increased motion). Additionally, the object used in this study requires relatively high grasp forces to break. Future investigations could focus on the role of object fragility in user preferences, where they may favor transmission configurations less sensitive to changes in input forces or motions when grasping more fragile objects.

Though the present work focuses primarily on body-powered systems in prostheses, further work could investigate the application of these findings to body-powered wearable orthoses. These devices, such as that presented in [39], hold the potential to aid individuals with other upper limb deficiencies like stroke and spinal cord injury. Additional studies could examine whether similar trends are seen in devices which operate with intact limbs, where findings could provide guidance for novel orthotic technologies.

V. Conclusion

In this work, we characterized the role of changing user forces and excursions on grasp performance and device sentiment. We used a custom emulator test bed to decouple force and position in body-powered grasping in order to systematically study the effect of each individually for the first time. This study showed that the separate effects found when isolating the roles of force and position help to explain the force-motion tradeoff when combined in a more realistic transmission configuration. Based on functional and qualitative results from a simulated grasping task, we found force, not position, to be the primary driver of functional performance, while both force and position affect user attitudes towards the device. From this, we present guidelines to aid the development of novel body-powered, shoulder-driven prostheses and orthoses that effectively address the force-motion tradeoff.

Appendix A
Participant Surveys

1) Post-Configuration Survey: (Q1) The task was easy to complete using the system in this configuration. (Q2) The system in this configuration was comfortable to operate. (Q3) Please rate your perceived exertion during the tasks with the system in this configuration.

2) Post-Block Survey: (Q1) Were there any conditions in this testing block that you preferred? What aspects contributed to that/those preference(s)? (Q2) Were there any conditions in this testing block that you particularly disliked? What aspects contributed to that/those dislike(s)? (Q3) Are there any additional comments or overall thoughts that you would like to share regarding this testing block?

Acknowledgment

The authors thank Richard Nguyen, the UCSF Department of Orthopaedic Surgery, and the Embodied Dexterity Group.

References

[1] F. Cordella et al., "Literature review on needs of upper limb prosthesis users," *Frontiers Neurosci.*, vol. 10, p. 209, May 2016.

[2] D. Datta, K. Selvarajah, and N. Davey, "Functional outcome of patients with proximal upper limb deficiency–acquired and congenital," *Clin. Rehabil.*, vol. 18, no. 2, pp. 172–177, Mar. 2004.

[3] E. A. Biddiss and T. T. Chau, "Upper limb prosthesis use and abandonment: A survey of the last 25 years," *Prosthetics Orthotics Int.*, vol. 31, no. 3, pp. 236–257, Sep. 2007.

[4] *Bebionic Hand*. Accessed: Oct. 28, 2020. [Online]. Available: https://www.ottobockus.com/prosthetics/upper-limb-prosthetics/solution-overview/bebionic-hand/

[5] *I-Limb Ultra*. Accessed: Oct. 28, 2020. [Online]. Available: https://www.ossur.com/en-us/prosthetics/arms/i-limb-ultra/prosthetics/arms/i-limb-ultra

[6] A. J. Spiers, J. Cochran, L. Resnik, and A. M. Dollar, "Quantifying prosthetic and intact limb use in upper limb amputees via egocentric video: An unsupervised, at-home study," *IEEE Trans. Med. Robot. Bionics*, vol. 3, no. 2, pp. 463–484, May 2021.

[7] E. Biddiss, D. Beaton, and T. Chau, "Consumer design priorities for upper limb prosthetics," *Disab. Rehabil., Assistive Technol.*, vol. 2, no. 6, pp. 346–357, Jan. 2007.

[8] H. J. Witteveen, H. S. Rietman, and P. H. Veltink, "Vibrotactile grasping force and hand aperture feedback for myoelectric forearm prosthesis users," *Prosthetics Orthotics Int.*, vol. 39, no. 3, pp. 204–212, Jun. 2015.

[9] J. L. Dideriksen, I. U. Mercader, and S. Dosen, "Closed-loop control using electrotactile feedback encoded in frequency and pulse width," *IEEE Trans. Haptics*, vol. 13, no. 4, pp. 818–824, Oct. 2020.

[10] S. Casini, M. Morvidoni, M. Bianchi, M. Catalano, G. Grioli, and A. Bicchi, "Design and realization of the CUFF–clenching upper-limb force feedback wearable device for distributed mechano-tactile stimulation of normal and tangential skin forces," in *Proc. IEEE/RSJ Int. Conf. Intell. Robots Syst. (IROS)*, Sep. 2015, pp. 1186–1193.

[11] K. R. Schoepp, M. R. Dawson, J. S. Schofield, J. P. Carey, and J. S. Hebert, "Design and integration of an inexpensive wearable mechanotactile feedback system for myoelectric prostheses," *IEEE J. Transl. Eng. Health Med.*, vol. 6, pp. 1–11, 2018.

[12] *Ability Hand*. Accessed: Jun. 16, 2023. [Online]. Available: https://www.psyonic.io/ability-hand

[13] J. F. Lehmann, "Orthotics for the wounded combatant," in *Textbook of Military Medicine, Part IV. Rehabilitation of the Injured Combatant*, vol. 2. Washington, DC, USA: Office of the Surgeon General, 1999, pp. 703–740.

[14] *Cable Routing to Capture 'Elbow Flexion' Control Motion*. Accessed: Apr. 7, 2023. [Online]. Available: https://www.trsprosthetics.com/wp-content/uploads/2018/02/Cable-Routing-Guide.pdf

[15] *Adult Grip Prehensors*. Accessed: Apr. 7, 2023. [Online]. Available: https://www.trsprosthetics.com/product/adult-grip-prehensors/

[16] D. C. Simpson, "The choice of control system for the multimovement prosthesis: Extended physiological proprioception (EPP)," in *The Control of Upper-Extremity Prostheses and Orthoses*. Springfield, IL, USA: Charles C. Thomas, 1974, pp. 146–150.

[17] J. D. Brown, T. S. Kunz, D. Gardner, M. K. Shelley, A. J. Davis, and R. B. Gillespie, "An empirical evaluation of force feedback in body-powered prostheses," *IEEE Trans. Neural Syst. Rehabil. Eng.*, vol. 25, no. 3, pp. 215–226, Mar. 2017.

[18] M. Hichert, D. A. Abbink, P. J. Kyberd, and D. H. Plettenburg, "High cable forces deteriorate pinch force control in voluntary-closing body-powered prostheses," *PLoS ONE*, vol. 12, no. 1, Jan. 2017, Art. no. e0169996.

[19] M. Hichert, A. N. Vardy, and D. Plettenburg, "Fatigue-free operation of most body-powered prostheses not feasible for majority of users with trans-radial deficiency," *Prosthetics Orthotics Int.*, vol. 42, no. 1, pp. 84–92, Feb. 2018.

[20] M. A. Gonzalez, C. Lee, J. Kang, R. B. Gillespie, and D. H. Gates, "Getting a grip on the impact of incidental feedback from body-powered and myoelectric prostheses," *IEEE Trans. Neural Syst. Rehabil. Eng.*, vol. 29, pp. 1905–1912, 2021.

[21] D. Chappell, Z. Yang, H. W. Son, F. Bello, P. Kormushev, and N. Rojas, "Towards instant calibration in myoelectric prosthetic hands: A highly data-efficient controller based on the Wasserstein distance," in *Proc. Int. Conf. Rehabil. Robot. (ICORR)*, Jul. 2022, pp. 1–6.

[22] A. Filatov and O. Celik, "Effects of body-powered prosthesis prehensor stiffness on performance in an object stiffness discrimination task," in *Proc. IEEE World Haptics Conf. (WHC)*, Jun. 2015, pp. 339–344.

[23] M. E. Abbott, J. D. Fajardo, H. W. Lim, and H. S. Stuart, "Kinesthetic feedback improves grasp performance in cable-driven prostheses," in *Proc. IEEE Int. Conf. Robot. Autom. (ICRA)*, May 2021, pp. 10551–10557.

[24] R. S. Johansson and G. Westling, "Roles of glabrous skin receptors and sensorimotor memory in automatic control of precision grip when lifting rougher or more slippery objects," *Exp. Brain Res.*, vol. 56, no. 3, pp. 550–564, Oct. 1984.

[25] G. Borg, *Borg's Perceived Exertion and Pain Scales*. Champaign, IL, USA: Human Kinetics, 1998.

[26] J. Pinheiro, D. Bates, S. DebRoy, and D. Sarkar. (2020). *Linear and Nonlinear Mixed Effects Models*. [Online]. Available: https://CRAN.R-project.org/package=nlme

[27] A. Bell, M. Fairbrother, and K. Jones, "Fixed and random effects models: Making an informed choice," *Quality Quantity*, vol. 53, no. 2, pp. 1051–1074, Mar. 2019.

[28] D. Bates, M. Mächler, B. Bolker, and S. Walker, "Fitting linear mixed-effects models Usinglme4," *J. Stat. Softw.*, vol. 67, no. 1, pp. 1–48, 2015.

[29] R. H. B. Christensen. (2022). *Ordinal—Regression Models for Ordinal Data*. [Online]. Available: https://CRAN.R-project.org/package=ordinal

[30] J. E. Taylor, G. A. Rousselet, C. Scheepers, and S. C. Sereno, "Rating norms should be calculated from cumulative link mixed effects models," *Behav. Res. Methods*, vol. 2022, pp. 1–12, Sep. 2022.

[31] R. V. Lenth. (2022). *Emmeans: Estimated Marginal Means, Aka Least- Squares Means*. [Online]. Available: https://CRAN.R-project.org/package=emmeans

[32] J. Monzée, Y. Lamarre, and A. M. Smith, "The effects of digital anesthesia on force control using a precision grip," *J. Neurophysiol.*, vol. 89, no. 2, pp. 672–683, Feb. 2003.

[33] H. Kinoshita, "Effect of gloves on prehensile forces during lifting and holding tasks," *Ergonomics*, vol. 42, no. 10, pp. 1372–1385, Oct. 1999.

[34] G. Smit and D. H. Plettenburg, "Efficiency of voluntary closing hand and hook prostheses," *Prosthetics Orthotics Int.*, vol. 34, no. 4, pp. 411–427, Dec. 2010.

[35] K. Matsushita, S. Shikanai, and H. Yokoi, "Development of drum CVT for a wire-driven robot hand," in *Proc. IEEE/RSJ Int. Conf. Intell. Robots Syst.*, Oct. 2009, pp. 2251–2256.

[36] K. W. O'Brien et al., "Elastomeric passive transmission for autonomous force-velocity adaptation applied to 3D-printed prosthetics," *Sci. Robot.*, vol. 3, no. 23, Oct. 2018, Art. no. eaau5543.

[37] M. E. Abbott, A. I. W. McPherson, W. O. Torres, K. Adachi, and H. S. Stuart, "Effect of variable transmission on body-powered prosthetic grasping," in *Proc. Int. Conf. Rehabil. Robot. (ICORR)*, Jul. 2022, pp. 1–6.

[38] A. Chadwell, L. Kenney, D. Howard, R. T. Ssekitoleko, B. T. Nakandi, and J. Head, "Evaluating reachable workspace and user control over prehensor aperture for a body-powered prosthesis," *IEEE Trans. Neural Syst. Rehabil. Eng.*, vol. 28, no. 9, pp. 2005–2014, Sep. 2020.

[39] L. Gerez, J. Chen, and M. Liarokapis, "On the development of adaptive, tendon-driven, wearable exo-gloves for grasping capabilities enhancement," *IEEE Robot. Autom. Lett.*, vol. 4, no. 2, pp. 422–429, Apr. 2019.